ARTICLE

3.0T MR Coronary Angiography after Arterial Switch Operation for Transposition of The Great Arteries—Gd-FLASH Versus Non-Enhanced SSFP. A Feasibility Study

Kathrine Rydén Suther[1,*], Charlotte de Lange[1,2], Henrik Brun[3], Rolf Svendsmark[1], Bac Nguyen[1], Stig Larsen[4], Bjarne Smevik[1], Arnt Eltvedt Fiane[5,6], Harald Lauritz Lindberg[6] and Einar Hopp[1]

[1]Department of Radiology, Division of Radiology and Nuclear Medicine, Oslo University Hospital, Rikshospitalet, Oslo, Norway

[2]Department of Paediatric Radiology and Clinical Physiology, Queen Silvia Children's hospital, Sahlgrenska University Hospital, Gothenburg, Sweden

[3]Department of Paediatric Cardiology, Division of Paediatric and Adolescent Medicine, Oslo University Hospital, Oslo, Norway

[4]Norwegian University of Life Sciences, Faculty of Veterinary Medicine, Centre for Epidemiology and Biostatistics, Campus Adamstuen, Oslo, Norway

[5]Faculty of Medicine, University in Oslo, Oslo, Norway

[6]Department of Cardiothoracic Surgery, Oslo University Hospital, Rikshospitalet, Oslo, Norway

*Corresponding Author: Kathrine Rydén Suther. Email: lensut@ous-hf.no

ABSTRACT

Background: Patency of the coronary arteries is an issue after reports of sudden cardiac death in patients with transposition of the great arteries (TGA) operated with arterial switch (ASO). Recent studies give rise to concern regarding the use of ionising radiation in congenital heart disease, and assessment of the coronary arteries with coronary MR angiography (CMRA) might be an attractive non-invasive, non-ionising imaging alternative in these patients. Theoretically, the use of 3.0T CMRA should improve the visualisation of the coronary arteries. The objective of this study was to assess feasibility of 3.0T CMRA at the coronary artery origins by comparing image quality with non-contrast CMRA in ASO TGA patients to healthy age-matched controls, and by comparing image quality with non-contrast CMRA to contrast enhanced CMRA in the patient group. **Material and methods:** Twelve patients, 9-15 years (mean 11.9 years, standard deviation 1.5 years), and 12 age-matched controls (mean 12.7 years, standard deviation 1.7 years) were examined with 3D balanced steady-state free precession (SSFP). Nine of twelve patients had Gadolinium-enhanced fast low-angle shot (Gd-FLASH) performed after SSFP. Image quality at the coronary artery origins was evaluated subjectively with a 10 cm figurative visual analogue scale (fVAS) and objectively by signal-to-noise and contrast-to-noise ratio (SNR, CNR). **Results:** All, but one, coronary artery origins were identified. No significant difference in image quality scores was found between patients and controls with SSFP (mean values 6.5 cm—9.1 cm in patients and 7.0 cm—8.0 cm in controls, p-values > 0.1). With SSFP, intra-observer fVAS mean score was 6.7 cm—8.6 cm and with Gd-FLASH 7.7 cm—8.7 cm. CNR was higher with Gd-FLASH ($p < 0.03$). Intra-observer agreement index (AI) with SSFP was moderate-to-good (0.43–0.71) and with Gd-FLASH good (0.64–0.79) in all origins. Inter-observer AI was good in the left main stem (LMS) with SSFP (0.65). With Gd-FLASH inter-observer AI was good in LMS (0.78) and moderate (0.5) in the left anterior descending artery, but lacking in the other origins though with a good agreement on Bland-Altman plots. **Conclusions:** Our findings indicate a better, more reproducible image quality with Gd-FLASH than with non-contrast SSFP CMRA on 3.0T for evaluation of the coronary artery origins in ASO TGA children and adolescents.

1 Introduction

In transposition of the great arteries (TGA) there is a ventricular-arterial discordance creating two independent circulatory systems. The current correction procedure of choice is arterial switch operation (ASO) performed in the early neonatal period, in which the great arteries are switched in position and the coronary arteries re-implanted. The survival rate is excellent, but stenosis and kinking at the coronary artery re-implantation site may occur. Coronary artery events have been reported with different frequencies, and concern regarding the coronary artery patency and disease at long term have been expressed, pointing out the need for follow-up and surveillance [1–6].

Conventional coronary angiography is considered the gold standard for diagnosing coronary artery disease, but the method is invasive and often requires general anaesthesia in the young. But, non-invasive methods like computed tomography (CT) and magnetic resonance imaging (MRI) have gained increasing attention. Nevertheless, individuals with congenital heart disease (CHD) is exposed to an increasing number of cardiac procedures with low-dose ionising radiation [7]. The most important contributors to the effective cumulative dose has been found to be conventional angiography and CT, and the level of exposure vary with the CHD complexity [8]. An association between incident cancer and exposure to cardiac procedures with low dose ionising radiation is shown in adults with CHD [9], and this emphasize the need for a non-invasive, non-ionising method to evaluate the coronary arteries [8,10].

MRI provides excellent tissue contrast and is superior to CT for assessing the myocardial morphology and function. Coronary MR angiography (CMRA) can be performed in several ways, both targeted on the coronary arteries and in whole-heart mode, as well as with or without administration of contrast agents. A prospective multi-center study showed that 3D segmented k-space gradient-echo MR angiography (MRA) at 1.5T when compared to conventional coronary angiography allowed accurate detection of disease in the proximal and middle coronary artery segments [11]. However, the most commonly used CMRA technique at 1.5T is balanced steady-state free precession (SSFP) [12,13]. The whole-heart CMRA (WH-CMRA) approach has been shown to enable visualisation of a longer vessel length with a total examination time less or at least comparable to the targeted coronary artery approach [14,15]. A study using SSFP with an intravascular contrast agent displayed significantly more side branches and longer vessel segments with WH-CMRA as compared to targeted CMRA [16]. Gadolinium-enhanced fast low-angle shot (Gd-FLASH) has also been used for WH-CMRA, but a study by Gweon et al. found no advantage of this sequence compared to SSFP on 1.5T [17]. Non-contrast enhanced CMRA has been performed on a 1.5T MR in TGA children corrected with ASO [18].

Theoretically, increased magnetic field strength will improve the visualisation of the coronary arteries due to higher signal-to-noise ratio (SNR), higher resonance frequency and altered relaxation times [19]. Higher SNR can be traded off for reduced scan time and/or improved spatial resolution. Using 3.0T for CMRA was long challenging due to issues related to the increased field strength and increased specific absorption rate (SAR) [19]. Stuber et al. showed that non–contrast CMRA, with a 3D segmented k-space gradient echo sequence, was feasible at 3.0T [20]. In a comparison of this sequence at 1.5T and 3.0T, Sommer et al found a significant increase in SNR and contrast-to-noise ratio (CNR) at 3.0T, but without significantly improved image quality [21]. Comparison of non-contrast enhanced SSFP at 1.5T to contrast-enhanced FLASH at 3.0T revealed better depiction of coronary segments with higher CNR and a

shorter acquisition time at 3.0T [22]. WH-CMRA with slow infusion of extravascular contrast media has been used at 3.0T [23], and Yang et al. were able to detect coronary artery stenosis with moderate specificity and high sensitivity when compared to conventional coronary angiography [24]. A more recent study revealed a sensitivity of 78.2% and a specificity of 75% for detecting clinically significant coronary artery stenosis at 3.0T [25], and a systematic review and meta-analysis found WH-CMRA to increase specificity, while contrast administration increased sensitivity for detecting coronary artery disease [26].

The purpose of this study was to assess the feasibility of 3.0T CMRA for the evaluation of the coronary artery origins by comparison of image quality of non-contrast enhanced SSFP in children/adolescents with ASO TGA to healthy age-correlated volunteers, and by comparing non-contrast enhanced SSFP WH-CMRA to slow infusion Gd-FLASH WH-CMRA in ASO TGA children/adolescents hypothesizing that non-contrast enhanced SSFP would give equal image quality to slow infusion Gd-FLASH. The comparison to healthy age-correlated individuals was performed to see whether the post-operative status in the coronary artery origin in ASO TGA would affect the image quality by itself.

2 Material and Methods

2.1 Ethics Statement

The study was approved by the local ethics committee for human research, the Norwegian South East Regional Committee for Medical and Health Research Ethics, and all subjects and their parents/caretakers gave their written, informed consent to participation. This study was performed in accordance with the 1964 Helsinki declaration and its later amendments. The trial registration of this study: ClinicalTrials. gov: NCT01916499.

2.2 Subjects

TGA patients, 9 years–15 years, corrected with ASO as neonates at our University Hospital were invited to the study. Twelve randomly chosen patients of both genders, two from each age cohort (one year of birth) were enrolled, six of each gender (mean age 11.9 years, standard deviation (SD) 1.5 years). All twelve underwent WH-CMRA with SSFP, while nine of these underwent Gd-FLASH as well. Additionally, 12 healthy, age-correlated individuals (mean 12.7 years, SD 1.7 years), eight girls and four boys, underwent WH-CMRA SSFP for comparison, but they did not receive contrast media due to ethical considerations. MRI was completed without general anaesthesia or any sedation.

2.3 MRI Protocol

Examinations were done head first, in supine position at a 3.0T MR Skyra unit (TIM 4G, Siemens Medical Solutions, Erlangen, Germany) using an 18-channel body array coil combined with a 32-channel spine array coil. Respiratory navigation gating 2D PACE and a 4-lead vector-electrocardiogram was used for gating purposes, meaning that the scan efficiency was patient dependent. The unit has a maximum strength of 45 mT/m with a slew rate of 200 T/m/s. B0 shim was used. Before WH-CMRA a cine true fast imaging with steady-state precession (trueFISP) image in a 4-chamber view was used to determine the longest rest period of the cardiac cycle, i.e., the period with the least motion of the right coronary artery, assuming that the left coronary artery would be in a relative motionless period as well. The acquisition window was adjusted individually and both sequences were performed free-breathing with respiratory navigator window 3.5 mm. SAR was limited to 4.0 W/kg.

2.3.1 Balanced Steady-State Free Precession (SSFP) CMRA

A coronal 3D whole-heart, fat saturated, respiratory-gated and ECG-triggered trueFISP was performed with the following imaging parameters: TR/TE = 239.92 ms/1.31 ms, flip angle 90°, no magnetisation preparation pulse, bandwidth 1502 Hz/Px, field of view 350 mm, matrix 208 × 187, and reconstructed voxel size 0.8 mm × 0.8 mm × 1.0 mm. Parallel imaging was used, GRAPPA pat 2. Acquired voxel size 1.87 × 1.68 × 2 (field of view (FOV) × frequency × slice thickness).

2.3.2 Gadolinium Enhanced Fast Low-Angle Shot (Gd-FLASH) CMRA

This was performed with a 3D whole-heart, fat saturated, respiratory-gated and ECG-triggered FLASH sequence during iv injection of Gadoterate meglumine (Dotarem®, Guerbet, Villepinte, France) 0.4 ml/kg, flow rate 0.15 ml/sec with a power injector (Medrad®, Bayer HealthCare, Whippany, NJ, USA) followed by an injection of 30 ml saline solution at the same flow rate. The scan started 15 seconds after initiating contrast media injection, and fulfilled sampling after completion of the contrast agent injection. The following imaging parameters were used: TR/TE = 345.04 ms/1.23 ms, flip angle 20°, non-selective IR preparation pulse, bandwidth 698 Hz/Px, field of view 320 mm, matrix 256 × 256, and reconstructed voxel size 0.6 mm × 0.6 mm × 0.9 mm. Parallel imaging was used, GRAPPA pat 2. Acquired voxel size 1.25 × 1.25 × 1.80 (FOV × frequency × slice thickness).

2.4 Data Analysis

Image post-processing was performed offline at a Vitrea work station (Toshiba Medical Systems, Tokyo, Japan), and evaluated by two radiologists with 3 years and 10 years of experience reading cardiac MRI, respectively. Readers were blinded for the examination group and any clinical symptoms. The first reader performed a second reading of the dataset 1 month apart from the first reading.

There are two complementary concepts used to assess image quality: qualitative/subjective analyses and quantitative/objective analyses. Qualitative/subjective image quality was used to assess the visibility/patency at the origin of the left main stem (LMS), left anterior descending artery (LAD), circumflex artery (CX) and right coronary artery (RCA) as well as determining the anatomical ostia and the identifiable length of the coronary arteries. Figurative visual analogue scale (fVAS) was used to score image quality subjectively [27]. fVAS is a line of pre-defined length with absolute minimum and maximum scores at the boundaries and with reference points in between them. A two-sided ruler with a sliding marker is used, where one side of the ruler has a 10 cm scale and the other side has a corresponding 10 cm plain, long line with reference points. The reference points and boundaries correspond to pre-defined image criteria (Tab. 1 and Fig. 1). Recordings were done by using the sliding marker on the side with the reference points, then turning the ruler to the opposite side to read out the corresponding score on the 10 cm scale with the help of the sliding marker. Satisfactory image quality for evaluating the origin of the coronary artery was set to fVAS ≥ 6.6 cm. In the case of a difference in score ≥ 3.5 cm between the two readers, an agreement was made upon consensus and the score with the biggest difference from the consensus score was changed.

Table 1: Reference points scoring criteria in figurative visual analogue scale

Reference point	Criteria
0 cm	Origin not visible/barely visible with highly blurred vessel wall
3.3 cm	Visible origin with moderately blurred vessel wall
6.6 cm	Origin with slightly blurred vessel wall
10 cm	Origin with excellently sharp defined vessel wall
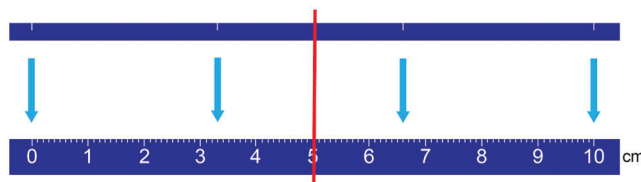
Figure 1: The two sides of the ruler for figurative visual analogue scale (fVAS) for qualitative image quality assessment. At the top: the plain side with a line with white reference marks (at 0, 3.3, 6.6 and 10 cm), and at the bottom: The corresponding 10 cm ruler at the opposite side. The red line illustrates the slider showing the corresponding points on both sides of the ruler

For quantitative/objective assessment, SNR and CNR were calculated using the axial multi-planar reconstruction (MPR) of the coronal SSFP sequence and the tilted axial MPR of the Gd-FLASH sequence to set a region of interest (ROI =15 mm²) in both myocardium (middle/apical part of the ventricular septum), air as well as in the origin of the coronary arteries. The ROI was made as large as possible within the borders of the origin of each coronary artery (LMS, LAD, CX, RCA), on an MPR projection perpendicular to the origin of the artery. The CNR and SNR were determined according to the following equations in which SI is signal intensity and SD is the standard deviation of the signal intensity:

$$CNR = \frac{SI_{\text{coronary artery}} - SI_{\text{myocardium}}}{SD_{\text{air}}}$$

$$SNR = \frac{\text{Mean } SI_{\text{coronary artery}}}{SD_{\text{air}}}$$

2.5 Statistical Analysis

Shapiro-Wilk test was performed for assumption of normal distribution [28]. Continuously distributed variables are expressed by mean values, standard deviation (SD) in brackets and 95% confidence intervals calculated by the Student's procedure [29]. Comparison within and between groups were performed by paired sample t-test and independent sample t-test, respectively [29]. Inter- and intra-observer agreement was calculated using Bland & Altman agreement analysis [30,31] including the calculation of the agreement index given by the formula:

$$AI = 1 - \frac{2SD(\text{difference between observations})}{\text{mean of observations}}$$

AI has the following levels of agreement: <0.20 poor, 0.21–0.40 fair, 0.41–0.60 moderate, 0.61–0.80 good, and 0.81–1.00 very good [29]. SPSS version 24 was used for performing the analyses (SPSS Inc., Chicago, USA). p-values < 0.05 were considered significant.

3 Results

There were six of each gender in the ASO TGA group, and eight girls and four boys in the control group, and the participant characteristics are shown in Tab. 2. All individuals had SSFP WH-CMRA performed and 9/12 patients had Gd-FLASH WH-CMRA performed.

All individuals completed the MRI exam without complications or complaints. In the patient group, mean acquisition time for SSFP was 5.7 minutes (SD 2.5 minutes) and for Gd-FLASH 7.1 minutes (SD 1.4 minutes). Some of the results in this article were previously reported as part of a different study exploring three different qualitative/subjective methods for image quality assessment [27].

The origin and proximal parts of the coronary arteries were identified, and as expected, the re-implanted ostia were located slightly cranial to the normal sinus position in healthy individuals. Tab. 3 shows the coronary artery pattern in the ASO TGA individuals. Seven patients had a normal coronary artery pattern post-ASO with the RCA ostium in the right sinus and the LMS ostium in the left sinus. In one individual CX was not recognised in the first reading and consequently interpreted/registered as invisible.

Table 2: Participant characteristics, and coronary arteries length and ostial area with steady-state free precession and gadolinium enhanced fast low angle shot

		Controls n = 12	TGA n = 12		p-value	
Age at exam (years)		12.7 (1.7)	11.9 (1.5)		0.3	
Male: Female		4:8	6:6		n/a	
Height (cm)		156.3 (13.1)	151.3 (9.8)		0.3	
Weight (kg)		44.5 (13.1)	41.2 (10.8)		0.5	
BSA (m^2)		1.38 (0.25)	1.31 (0.21)		0.5	
MR sequence		SSFP n = 12	SSFP n = 12	Gd-FLASH n = 9	**Controls vs TGA** SSFP	**TGA** SSFP vs Gd-FLASH
LMS	Area (mm^2)	13.2 (4.6)	12.1 (5.7)	8.3 (3.3)	0.7	0.4
	Length (cm)	0.8 (0.2)	1.1 (0.6)	1.3 (0.5)	0.2	0.8
LAD	Area (mm^2)	9.4 (2.9)	7.7 (2.7)	5.4 (2.2)	0.1	**0.03**
	Length (cm)	4.8 (2.7)	5.1 (2.6)	6.5 (3.5)	0.8	0.2
CX	Area (mm^2)	8.6 (2.5)	6.5 (3.0)	5.1 (2.5)	0.08	0.1
	Length (cm)	2.8 (1.7)	2.0 (1.6)	2.4 (1.8)	0.3	0.4
RCA	Area (mm^2)	13.7 (4.4)	15.8 (9.0)	8.4 (4.0)	0.5	**0.02**
	Length (cm)	6.5 (3.8)	8.1 (3.3)	8.0 (1.8)	0.3	0.9

TGA = transposition of the great arteries; n = number of individuals; BSA = body surface area; SSFP = steady-state free precession; Gd-FLASH = Gadolinium-enhanced fast low-angle shot; LMS = left main stem; LAD = left anterior descending artery; CX = circumflex artery; RCA = right coronary artery. Mean values with standard deviation in brackets. p-values ≤ 0.05 were considered statistically significant (bold).

Table 3: Coronary artery pattern after arterial switch operation in the patients

Left sinus	Right sinus	n
LMS	RCA	7
LAD	RCA + CX	4[*][^]
LAD + RCA	CX	1[*]

n = number of patients; LMS = left main stem; RCA = right coronary artery; LAD = left anterior descending artery; CX = circumflex artery. *no LMS was defined. ^in one patient CX was not recognised and interpreted as invisible.

In addition, CX was not identified in one healthy volunteer and hence no LMS was defined, but otherwise there was a normal coronary artery pattern in the healthy volunteers. In those individuals with common ostia (RCA and CX or RCA and LAD) the origin of the different coronary arteries was evaluated separately. This resulted in a total of 88 coronary origins identified with SSFP (24 individuals) and 33 with Gd-FLASH (9 patients) (Tab. 4).

There was no significant difference in identifiable length measured on multi-planar reconstructions of SSFP and Gd-FLASH in the patient group, p > 0.2 (Tab. 2). The range of image quality of the coronary artery origin with SSFP and Gd-FLASH are illustrated in Fig. 2.

Table 4: Figurative visual analogue scale reader agreement

	Variable	Intra (within observer)				Inter (between observers)			
		LMS	LAD	CX	RCA	LMS	LAD	CX	RCA
SSFP	Mean score (cm)	6.7 (1.4)	6.8 (1.8)	6.9 (1.7)	8.6 (1.8)	7.0 (1.2)	6.6 (2.0)	6.2 (1.9)	7.7 (2.1)
	Mean diff	0.6 (1.4)	0.4 (1.9)	0.0 (1.4)	0.0 (1.2)	0.1 (1.2)	0.8 (1.6)	1.4 (1.2)	1.8 (0.7)
	AI	0.59	0.43	0.61	0.71	0.65	0.51	0.61	0.82
	Outliers	1/18	1/24	1/22	1/24	0/18	1/24	1/22	0/24
Gd-FLASH	Mean score (cm)	7.7 (1.7)	8.0 (2.4)	7.7 (2.2)	8.7 (1.6)	7.7 (1.6)	7.3 (2.4)	7.0 (2.1)	8.3 (1.5)
	Mean diff	0.7 (0.8)	−0.4 (1.4)	0.0 (0.8)	0.0 (1.0)	0.8 (0.9)	1.0 (1.8)	1.6 (1.3)	0.8 (0.7)
	AI	0.79	0.64	0.79	0.78	0.78	0.50	0.64	0.83
	Outliers	0/6	0/9	0/9	1/9	0/6	1/9	0/9	0/9

LMS = left main stem; LAD = left anterior descending artery; CX = circumflex artery; RCA = right coronary artery; SSFP = steady-state free precession; Gd-FLASH = Gadolinium-enhanced fast low-angle shot; AI = agreement index. Standard deviation in brackets.

(a)   (b)
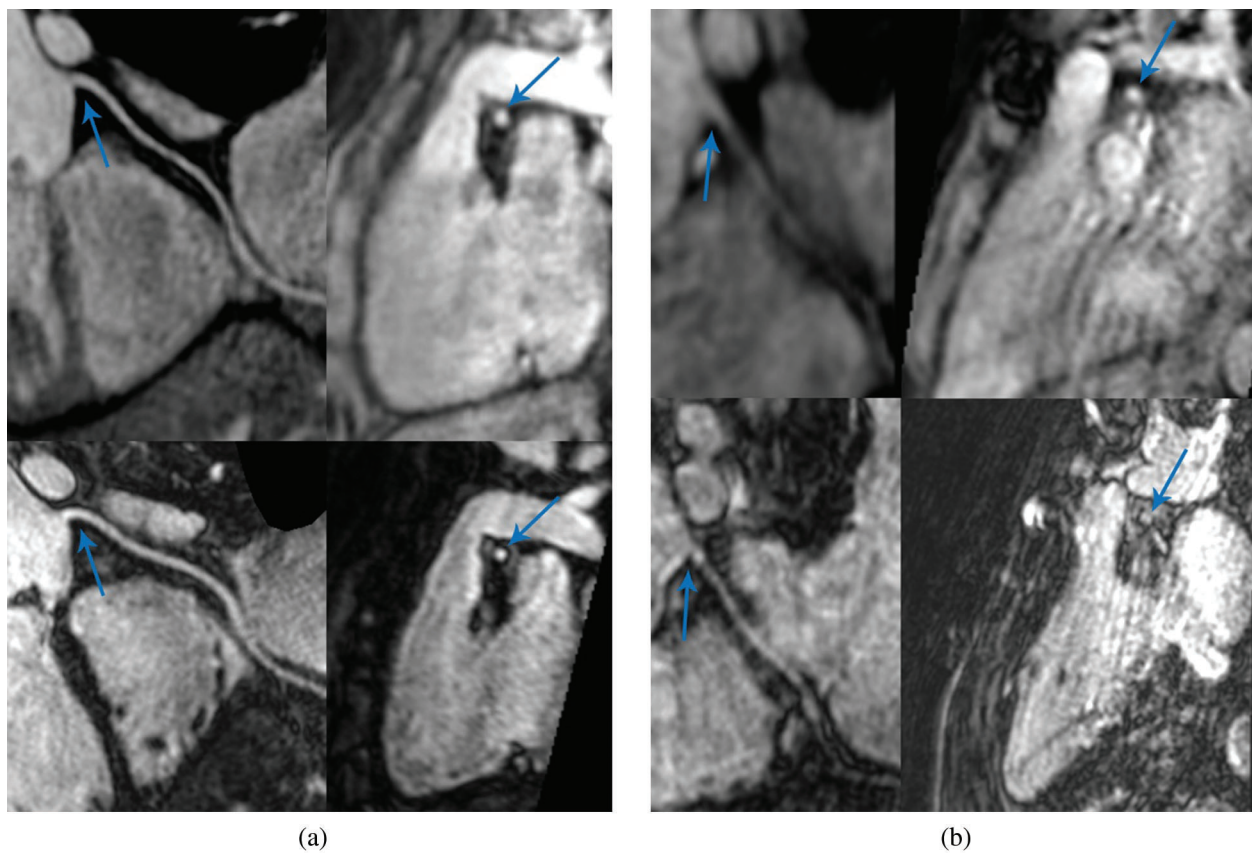
Figure 2: Coronary magnetic resonance angiography (CMRA). Multi-planar reconstruction (MPR) of the right coronary artery (RCA). (a) Shows a fourteen-year-old female patient with very good image quality. (b) Shows an eleven-year-old male patient with suboptimal image quality. In both images; Upper row: RCA reconstruction of steady-state free precession to the left and cross-section of the RCA ostium to the right (arrow). Lower row: RCA reconstruction of Gadolinium-enhanced fast low-angle shot to the left and cross-section of the RCA ostium to the right (arrow)

There was no significant difference in subjective image quality when comparing the scores in healthy volunteers to TGA patients with SSFP, but when comparing the scores with SSFP to Gd-FLASH in TGA patients there was a significant difference in the scores for CX ($p = 0.05$) (Tab. 5).

Table 5: Figurative visual analogue scale, subjective image quality assessment results for observer 1, first reading

|	Group	MR sequence	n	fVAS			
				Mean score in cm (SD)	95% Confidence Interval	*p*-value SSFP, controls *vs.* TGA	*p*-value TGA, SSFP *vs.* Gd-FLASH
LMS	Controls	SSFP	11	7.0 (1.0)	6.3–7.6	0.8	0.1
	TGA	SSFP	7	7.1 (1.1)	6.0–8.1		
		Gd-FLASH	6	8.1 (1.6)	6.4–9.8		
LAD	Controls	SSFP	12	7.3 (1.8)	6.2–8.5	0.3	0.5
	TGA	SSFP	12	6.6 (1.9)	5.4–7.8		
		Gd-FLASH	9	7.8 (2.7)	5.7–9.9		
CX	Controls	SSFP	11	7.3 (1.7)	6.2–8.4	0.2	**0.05**
	TGA	SSFP	11	6.5 (1.6)	5.3–7.6		
		Gd-FLASH	9	7.7 (2.1)	6.1–9.4		
RCA	Controls	SSFP	12	8.0 (2.4)	6.5–9.5	0.1	0.7
	TGA	SSFP	12	9.1 (0.9)	8.5–9.7		
		Gd-FLASH	9	8.7 (1.3)	7.7–9.7		

fVAS = figurative visual analogue scale; n = number of individuals; SD = standard deviation; SSFP = steady-state free precession; TGA = transposition of the great arteries; Gd-FLASH = Gadolinium enhanced fast low-angle shot; LMS = left main stem; LAD = left anterior descending artery; CX = circumflex artery; RCA = right coronary artery. *p*-values ≤ 0.05 were considered statistically significant (bold).

The intra-observer AI for SSFP was moderate in LMS and LAD and good in CX and RCA, while the inter-observer AI was good in LMS (Tab. 4). The agreement analysis could not be used for inter-observer agreement in LAD, CX and RCA because of significant difference in scoring between the two readers, but Bland-Altman plots showed a good agreement (Fig. 3). On Gd-FLASH a good intra-observer AI was found in all four origins, and there was a good inter-observer AI in LMS and moderate AI in LAD (Tab. 4). However, the agreement analysis could not be used for CX and RCA owing to significant difference in scoring between the two readers. Nevertheless, the Bland-Altman plots showed a good agreement between the two readers (Fig. 4). Reader 2 scored significantly lower than reader 1 on both SSFP and Gd-FLASH when AI could not be used.

For the objective image quality, CNR was higher in all coronary artery origins on Gd-FLASH compared to SSFP $p \leq 0.03$ (Tab. 6).

The area of the origin was significantly smaller with Gd-FLASH in LAD and RCA compared to SSFP, respectively, $p = 0.02$ and $p = 0.03$ (Tab. 2).
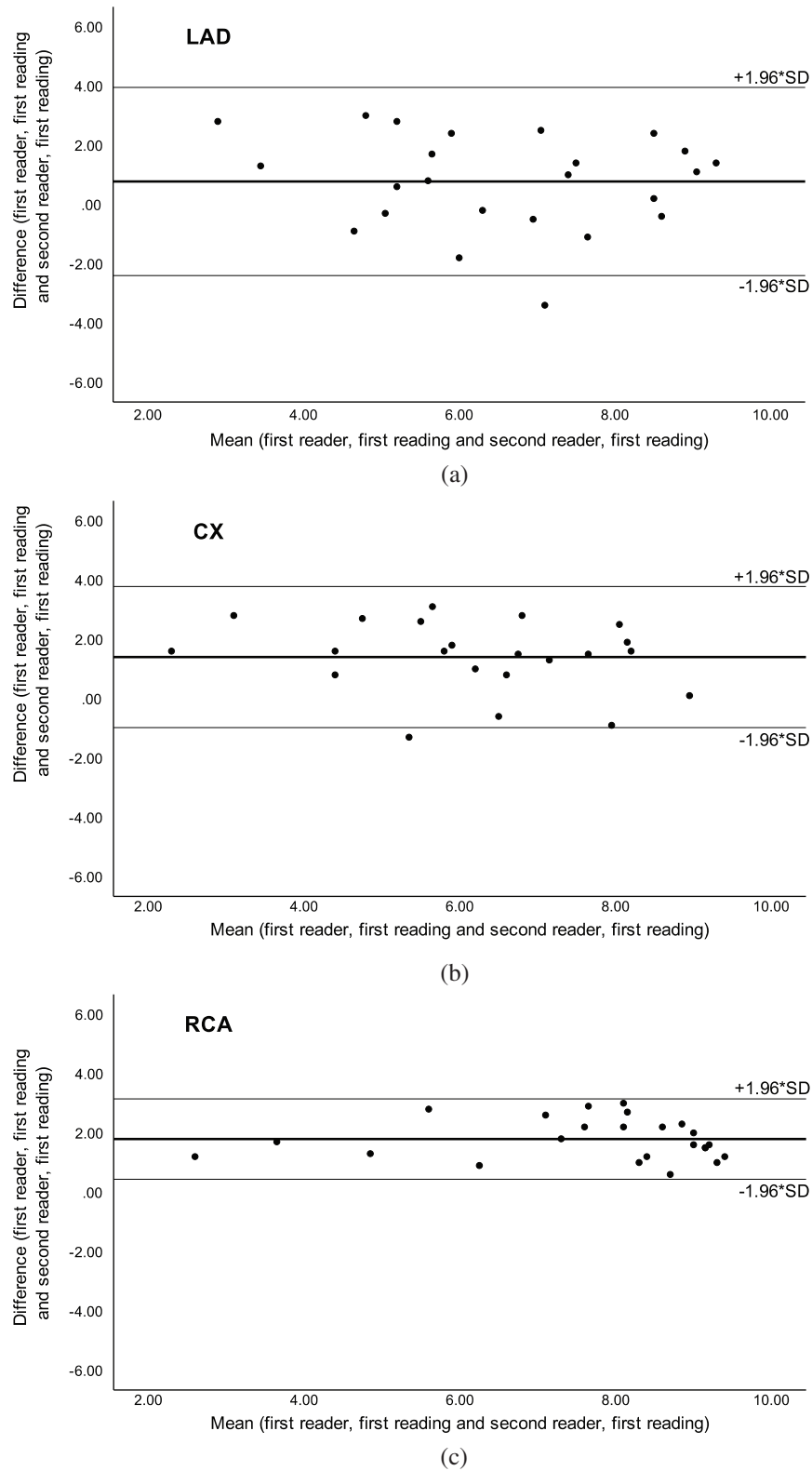
Figure 3: Bland-Altman plots of inter-observer agreement with steady-state free precession (SSFP) for the a) left anterior descending artery (LAD), b) circumflex artery (CX) and c) right coronary artery (RCA). Adapted with permission from [27]

(a)

(b)
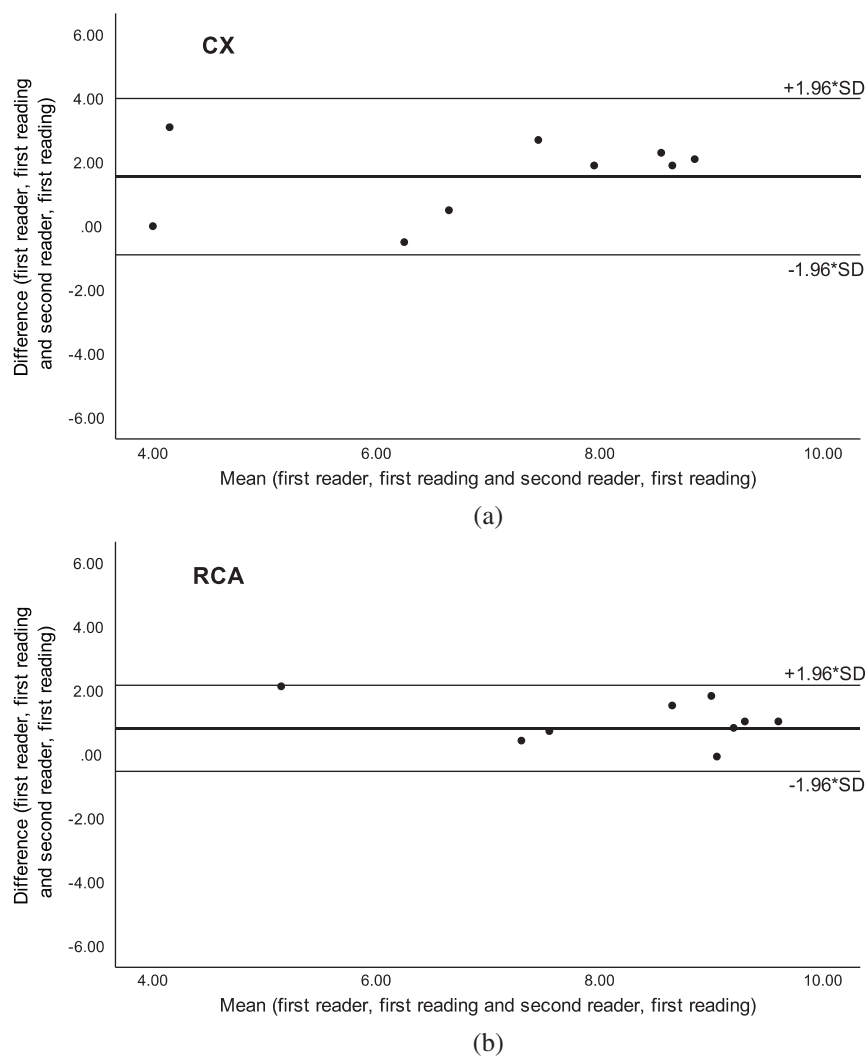
Figure 4: Bland-Altman plots of inter-observer agreement with Gadolinium-enhanced fast low-angle shot (Gd-FLASH) for the a) circumflex artery (CX) and b) right coronary artery (RCA)

Table 6: Objective image quality assessment

Variable	n	Gd-FLASH	SSFP	Mean difference Gd-FLASH-SSFP	p-value
SNR LMS	6	97.3 (32.2)	83.4 (51.1)	13.9 (-70.4–98.3)	0.69
SNR LAD	9	108.0 (55.1)	61.6 (39.6)	46.4 (-15.6–108.4)	0.12
SNR RCA	9	95.4 (35.6)	77.8 (37.9)	17.6 (-26.2–61.4)	0.38
SNR CX	9	90.1 (42.4)	61.1 (41.7)	29.0 (-20.6–78.5)	0.21
CNR LMS	6	75.0 (31.2)	23.2 (14.8)	51.8 (9.1–94.5)	**0.03**
CNR LAD	9	85.5 (51.5)	5.2 (16.9)	80.3 (37.8–122.7)	**<0.01**
CNR RCA	9	72.9 (29.1)	21.4 (10.6)	51.5 (30.1–72.9)	**<0.01**
CNR CX	9	67.6 (39.4)	4.7 (20.0)	62.9 (33.4–92.4)	**<0.01**

n = number of individuals; Gd-FLASH = Gadolinium-enhanced fast low-angle shot; SSFP = steady-state free precession; SNR = signal-to-noise ratio; LMS = left main stem; LAD = left anterior descending artery; CX = circumflex artery; RCA = right coronary artery; CNR contrast-to-noise ratio. Mean values with standard deviation and 95% confidence intervals in brackets. p-values ≤ 0.05 were considered statistically significant (bold).

4 Discussion

In this study, we have performed WH-CMRA at 3.0T MR comparing two different sequences, without (SSFP) and with contrast-enhancement (Gd-FLASH), for assessment of the coronary artery origins in TGA children/adolescents with ASO and age-matched controls. We found that the image quality of the coronary artery origin was rated, in most cases, to be sufficient or superior (fVAS ≥ 6.6 cm) when using Gd-FLASH, while the image quality with SSFP, in general, was sufficient or superior, but had an inferior intra- and inter-observer AI.

The scan time for Gd-FLASH WH-CMRA was in the same range as shown in other studies with contrast-enhanced WH-CMRA at 3.0T [22,24], while the scan time for SSFP WH-CMRA was clearly shorter than reported in studies performed at 1.5T [17,22].

Coronary artery pattern was identified in all patients and controls, and we found similar results as Taylor et al. regarding the visualised coronary artery length [18].

Sufficient or better image quality score was found in 62/88 (70%) coronary origins with SSFP. These findings are comparable to a study at 1.5T on a similar patient group with targeted non-contrast CMRA where diagnostic quality images were achieved in 72% [18]. In our study, Gd-FLASH, in general, improved the visualisation, and 26/33 (79%) coronary artery origins had a fVAS score ≥ 6.6 cm compared to 22/33 (67%) with SSFP. This is in contradiction to the study at 1.5T by Gweon et al. where Gd-FLASH did not improve image quality [17]. However, they evaluated the whole length of the coronary arteries and in addition used a 5-point categorical scale for subjective quality assessment which might be disadvantageous in the assessment from a statistical point of view as there is a tendency to choose the central measure being a geometric mean or median and not the parametric mean [32]. On the other hand, when comparing SSFP versus Gd-FLASH on an individual basis, no statistically significant difference was found, probably explained by a low sample size in our study.

A 10 cm VAS was used for subjective image quality scoring as reported in a few other studies [33,34], but in our study reference points were added to the ruler, fVAS [27]. Traditionally, fixed point scale has been used in most other coronary artery studies and radiological studies [17,21–24,35], but as subjective image quality tends to vary along a continuum, the use of a fixed-point scale for image quality assessment, could potentially reduce the informative value of the scoring especially in small sample size studies. Both the intra- and inter-observer AI were clearly better for Gd-FLASH compared to SSFP. However, the agreement index could not be used for some origins due to significant difference in scores between the two readers. This could be explained by the longer experience of the second reader (10 years) compared to the first reader (3 years) since there was no significant difference in the two readings done by the first reader permitting calculation of intra-observer AI. The Bland-Altman plots revealed a systematic difference between the readers supporting that this could be explained by reader experience.

In general, the area of the coronary artery origin with Gd-FLASH was smaller than with SSFP, even though the difference was not significant for all origins probably due to a low patient number. There are several possible explanations for this as well as the improved intra- and inter-observer AI with Gd-FLASH. The acquired spatial resolution of the two different sequences were different, and this can cause differences in measurement and perception of the images. SSFP is a sequence sensitive to increased magnetic field inhomogeneity and frequency offset from tissue susceptibility variation found in higher field strength [19], and image quality is variable [36]. Spoiled gradient-echo sequences are less sensitive to field inhomogeneity, but the blood-myocardial contrast and SNR of the coronary arteries are not as high as those from SSFP, and with these sequences T1-shortening contrast agents must be used [19]. As a gradient echo sequence, FLASH has a higher signal than SSFP at 3.0T, and the use of an intravascular contrast agent together with an inversion recovery preparation pulse have been shown to improve SNR and CNR [19]. Therefore, a better delineation of the vessel and ostia can be achieved.

The spatial resolution achieved with CT images is better than with MRI, and in addition, there is a challenge with the performance of CMRA in the presence of a high heart rate. Some of the known complications of ASO for TGA like pulmonary and branch pulmonary artery stenosis and coronary artery issues [4] may require imaging with CT angiography and cardiac catheterisation with intervention. Technical improvements with introduction of dual-source CT, low voltage imaging, high pitch factors and iterative reconstruction as well as prospective ECG triggering have led to reduction of radiation dose [37–42]. Nevertheless, the United Nations Scientific Committee on the Effects of Atomic Radiation (UNSCEAR) report 2013, notes that children are clearly more radiosensitive for some types of tumours than adults [43], and non-ionising diagnostic imaging is an advantage when possible to use. In general, individuals with CHD are exposed to a higher level of ionising radiation than the normal population, but the level of exposure varies greatly with the complexity of congenital heart disease [8]. A recent study showed an association between cancer incident and low dose ionising radiation in adults with CHD [9], and this emphasise the importance of non-ionising diagnostic imaging in CHD patients.

Over the past couple of years concern has been raised regarding Gd deposition in brain after Gd exposure even though the clinical significance of this remains unknown [44]. However, this calls for cautious use especially in patients who might need several exams throughout life.

Current guidelines recommend regularly follow-up with echocardiography and CMR [4,45–47], and an anatomical evaluation of coronary artery patency has been found sensible in asymptomatic adults even though there is no consensus regarding what modality should be used. On the other hand, the recent guideline from the European Society of Cardiology (ESC) questions whether routine screening of the coronary arteries in asymptomatic adults with ASO TGA can be justified as the incidence of late coronary artery related issues is low [45]. Still, a non-ionising, promising, non-invasive technique for visualisation of the proximal coronary arteries, could be an important supplement in the routine follow-up, given the additional information provided by CMR on myocardial function, vascular flow and tissue characterisation, to identify long-term complications, and to identify individuals in need of further coronary artery diagnostic follow-up and surveillance.

5 Limitations

We acknowledge some limitations of our study. First, we were not able to compare the diagnostic quality to CT coronary angiography or to the gold standard: conventional coronary angiography. Using ionising techniques in paediatric patients is controversial unless there is a medical indication for performing such an examination, and this would not have been approved by the ethics committee with the current recommendations on follow-up in this patient group. Second, in this feasibility study, the patient number is low, meaning that small changes in the grading of the coronary artery origin in one individual will potentially result in great differences. Thirdly, the ideal age for assessment of the coronary arteries in the ASO TGA group might be younger than in our cohort, maybe before the child starts practicing sports. However, there is a debate regarding the need for early coronary assessment. Imaging small children can be very challenging with the potential need of sedation/general anaesthesia, but also due to an expected physiological increased heart rate and respiratory rate. Because of the above-mentioned issues and the expected smaller size of the coronary arteries, CMRA at 3.0T in the younger children is technically very challenging. Fourthly, for ethical reasons we could not compare 3.0T Gd-FLASH to 1.5T SSFP which would have added strength to the study. Finally, we only evaluated the origin of the coronary arteries, as this is the crucial area in the re-implanted coronary arteries in these patients with a risk of kinking and stenosis. Whether Gd-FLASH can be used for evaluating the coronary arteries along their course peripherally in this patient group has not been assessed.

6 Conclusions

In our study of children/adolescents with TGA and ASO, the use of Gd-FLASH WH-CMRA on 3.0T for assessment of the coronary artery origins, provided sufficient-to-good image quality, while non-contrast enhanced CMRA, SSFP, seems less reliable. Addition of coronary MRA to the CMR follow-up of ASO TGA patients could have a role in identifying individuals in need of further coronary artery diagnostic work-up and surveillance before the age where manifestation of acquired coronary artery disease potentially occur.

Conflicts of Interest: The authors declare that they have no conflicts of interest to report regarding the present study.

References

1. Bonnet, D., Bonhoeffer, P., Piechaud, J. F., Aggoun, Y., Sidi, D. et al. (1996). Long-term fate of the coronary arteries after the arterial switch operation in newborns with transposition of the great arteries. *Heart, 76(3),* 274–279. DOI 10.1136/hrt.76.3.274.

2. Cohen M. S., Wernovsky G. (2006). Is the arterial switch operation as good over the long term as we thought it would be?. *Cardiology in the Young, 16(S3),* 117–124. DOI 10.1017/S1047951106001041.

3. Hauser, M., Bengel, F. M., Kuhn, A., Sauer, U., Zylla, S. et al. (2001). Myocardial blood flow and flow reserve after coronary reimplantation in patients after arterial switch and ross operation. *Circulation, 103(14),* 1875–1880. DOI 10.1161/01.CIR.103.14.1875.

4. Cohen, M. S., Eidem, B. W., Cetta, F., Fogel, M. A., Frommelt, P. C. et al. (2016). Multimodality imaging guidelines of patients with transposition of the great arteries: A report from the American society of echocardiography developed in collaboration with the society for cardiovascular magnetic resonance and the society of cardiovascular computed tomography. *Journal of the American Society of Echocardiography, 29(7),* 571–621. DOI 10.1016/j.echo.2016.04.002.

5. Hutter, P. A., Kreb, D. L., Mantel, S. F., Hitchcock, J. F., Meijboom, E. J. et al. (2002). Twenty-five years' experience with the arterial switch operation. *Journal of Thoracic and Cardiovascular Surgery, 124(4),* 790–797. DOI 10.1067/mtc.2002.120714.

6. Pasquali, S. K., Hasselblad, V., Li, J. S., Kong, D. F., Sanders, S. P. (2002). Coronary artery pattern and outcome of arterial switch operation for transposition of the great arteries: A meta-analysis. *Circulation, 106(20),* 2575–2580. DOI 10.1161/01.CIR.0000036745.19310.BB.

7. Beauséjour Ladouceur, V., Lawler, P. R., Gurvitz, M., Pilote, L., Eisenberg, M. J. et al. (2016). exposure to low-dose ionizing radiation from cardiac procedures in patients with congenital heart disease: 15-year data from a population-based longitudinal cohort. *Circulation, 133(1),* 12–20. DOI 10.1161/CIRCULATIONAHA.115.019137.

8. Johnson, J. N., Hornik, C. P., Li, J. S., Benjamin, D. K., Yoshizumi, T. T. et al. (2014). Cumulative radiation exposure and cancer risk estimation in children with heart disease. *Circulation, 130(2),* 161–167. DOI 10.1161/CIRCULATIONAHA.113.005425.

9. Cohen, S., Liu, A., Gurvitz, M., Guo, L., Therrien, J. et al. (2018). Exposure to low-dose ionizing radiation from cardiac procedures and malignancy risk in adults with congenital heart disease. *Circulation, 137(13),* 1334–1345. DOI 10.1161/CIRCULATIONAHA.117.029138.

10. Ait-Ali, L., Andreassi, M. G., Foffa, I., Spadoni, I., Vano, E. et al. (2010). Cumulative patient effective dose and acute radiation-induced chromosomal DNA damage in children with congenital heart disease. *Heart, 96(4),* 269–274. DOI 10.1136/hrt.2008.160309.

11. Kim, W. Y., Danias, P. G., Stuber, M., Flamm, S. D., Plein, S. et al. (2001). Coronary magnetic resonance angiography for the detection of coronary stenoses. *New England Journal of Medicine, 345(26),* 1863–1869. DOI 10.1056/NEJMoa010866.

12. Deshpande, V. S., Shea, S. M., Laub, G., Simonetti, O. P., Finn, J. P. et al. (2001). 3D magnetization-prepared true-FISP: A new technique for imaging coronary arteries. *Magnetic Resonance in Medicine, 46(3),* 494–502. DOI 10.1002/mrm.1219.

13. Weber, O. M., Pujadas, S., Martin, A. J., Higgins, C. B. (2004). Free-breathing, three-dimensional coronary artery magnetic resonance angiography: Comparison of sequences. *Journal of Magnetic Resonance Imaging, 20(3),* 395–402. DOI 10.1002/jmri.20141.

14. Weber, O. M., Martin, A. J., Higgins, C. B. (2003). Whole-heart steady-state free precession coronary artery magnetic resonance angiography. *Magnetic Resonance in Medicine, 50(6),* 1223–12283. DOI 10.1002/mrm.10653.

15. Bi, X., Deshpande, V., Carr, J., Li, D. (2006). Coronary artery magnetic resonance angiography (MRA): A comparison between the whole-heart and volume-targeted methods using a T2-prepared SSFP sequence. *Journal of Cardiovascular Magnetic Resonance, 8(5),* 703–707. DOI 10.1080/10976640600723706.

16. Tang, L., Merkle, N., Schar, M., Korosoglou, G., Solaiyappan, M. et al. (2009). Volume-targeted and whole-heart coronary magnetic resonance angiography using an intravascular contrast agent. *Journal of Magnetic Resonance Imaging, 30(5),* 1191–1196. DOI 10.1002/jmri.21903.

17. Gweon, H. M., Kim, S. J., Lee, S. M., Hong, Y. J., Kim, T. H. (2011). 3D whole-heart coronary MR angiography at 1.5T in healthy volunteers: Comparison between unenhanced SSFP and Gd-enhanced FLASH sequences. *Korean Journal of Radiology, 12(6),* 679–685. DOI 10.3348/kjr.2011.12.6.679.

18. Taylor, A. M., Dymarkowski, S., Hamaekers, P., Razavi, R., Gewillig, M. et al. (2005). MR coronary angiography and late-enhancement myocardial MR in children who underwent arterial switch surgery for transposition of great arteries. *Radiology, 234(2),* 542–547. DOI 10.1148/radiol.2342032059.

19. Rajiah, P., Bolen, M. A. (2014). Cardiovascular MR imaging at 3T: Opportunities, challenges, and solutions. *RadioGraphics, 34(6),* 1612–1635. DOI 10.1148/rg.346140048.

20. Stuber, M., Botnar, R. M., Fischer, S. E., Lamerichs, R., Smink, J. et al. (2002). Preliminary report on *in vivo* coronary MRA at 3 Tesla in humans. *Magnetic Resonance in Medicine, 48(3),* 425–429. DOI 10.1002/mrm.10240.

21. Sommer, T., Hackenbroch, M., Hofer, U., Schmiedel, A., Willinek, W. A. et al. (2005). Coronary MR angiography at 3.0T versus that at 1.5T: Initial results in patients suspected of having coronary artery disease. *Radiology, 234(3),* 718–725. DOI 10.1148/radiol.2343031784.

22. Liu, X., Bi, X., Huang, J., Jerecic, R., Carr, J. et al. (2008). Contrast-enhanced whole-heart coronary magnetic resonance angiography at 3.0T: Comparison with steady-state free precession technique at 1.5 T. *Investigative Radiology, 43(9),* 663–668. DOI 10.1097/RLI.0b013e31817ed1ff.

23. Bi, X., Carr, J. C., Li, D. (2007). Whole-heart coronary magnetic resonance angiography at 3 Tesla in 5 minutes with slow infusion of Gd-BOPTA, a high-relaxivity clinical contrast agent. *Magnetic Resonance in Medicine, 58(1),* 1–7. DOI 10.1002/mrm.21224.

24. Yang, Q., Li, K., Liu, X., Bi, X., Liu, Z. et al. (2009). Contrast-enhanced whole-heart coronary magnetic resonance angiography at 3.0-T: A comparative study with X-ray angiography in a single center. *Journal of the American College of Cardiology, 54(1),* 69–76. DOI 10.1016/j.jacc.2009.03.016.

25. He, Y., Pang, J., Dai, Q., Fan, Z., An, J. et al. (2017). Diagnostic performance of self-navigated whole-heart contrast-enhanced coronary 3-T MR angiography. *Radiology, 283(3),* 923. DOI 10.1148/radiol.2017174013.

26. Di Leo, G., Fisci, E., Secchi, F., Ali, M., Ambrogi, F. et al. (2016). Diagnostic accuracy of magnetic resonance angiography for detection of coronary artery disease: A systematic review and meta-analysis. *European Radiology, 26(10),* 3706–3718. DOI 10.1007/s00330-015-4134-0.

27. Suther, K. R., Hopp, E., Smevik, B., Fiane, A. E., Lindberg, H. L. et al. (2018). Can visual analogue scale be used in radiologic subjective image quality assessment? *Pediatric Radiology, 48(11),* 1567–1575. DOI 10.1007/s00247-018-4187-8.

28. Shapiro, S. S., Wilk, M. B. (1965). An analysis of variance test for normality (complete samples). *Biometrika, 52(3–4),* 591–611. DOI 10.1093/biomet/52.3-4.591.

29. Altman, D. G. (1991). *Practical statistics for medical research*. London: Chapman and Hall.

30. Altman, D. G., Bland, J. M. (1983). Measurement in medicine: The analysis of method comparison studies. *Journal of the Royal Statistical Society Series D (The Statistician), 32(3),* 307–317.

31. Bland, J. M., Altman, D. G. (1986). Statistical methods for assessing agreement between two methods of clinical measurement. *Lancet (London, England), 327(8476),* 307–310. DOI 10.1016/S0140-6736(86)90837-8.

32. Stengel, D., Ottersbach, C., Kahl, T., Nikulka, C., Güthoff, C. et al. (2014). Dose reduction in whole-body computed tomography of multiple injuries (DoReMI): Protocol for a prospective cohort study. *Scandinavian Journal of Trauma, Resuscitation and Emergency Medicine, 22(1),* e442. DOI 10.1186/1757-7241-22-15.

33. Rienmüller, R., Brekke, O., Kampenes, V. B., Reiter, U. (2001). Dimeric versus monomeric nonionic contrast agents in visualization of coronary arteries. *European Journal of Radiology, 38(3),* 173–178. DOI 10.1016/S0720-048X(01)00304-7.

34. Stengel, D., Mutze, S., Güthoff, C., Weigeldt, M., von Kottwitz, K. et al. (2020). Association of low-dose whole-body computed tomography with missed injury diagnoses and radiation exposure in patients with blunt multiple trauma. *JAMA Surgery, 155(3),* 224–232. DOI 10.1001/jamasurg.2019.5468.

35. Miéville, F. A., Berteloot, L., Grandjean, A., Ayestaran, P., Gudinchet, F. et al. (2013). Model-based iterative reconstruction in pediatric chest CT: Assessment of image quality in a prospective study of children with cystic fibrosis. *Pediatric Radiology, 43(5),* 558–567. DOI 10.1007/s00247-012-2554-4.

36. Bi, X., Deshpande, V., Simonetti, O., Laub, G., Li, D. (2005). Three-dimensional breathhold SSFP coronary MRA: A comparison between 1.5T and 3.0T. *Journal of Magnetic Resonance Imaging, 22(2),* 206–212. DOI 10.1002/jmri.20374.

37. Gao, W., Zhong, Y. M., Sun, A. M., Wang, Q., Ouyang, R. Z. et al. (2016). Diagnostic accuracy of sub-mSv prospective ECG-triggering cardiac CT in young infant with complex congenital heart disease. *International Journal of Cardiovascular Imaging, 32(6),* 991–998. DOI 10.1007/s10554-016-0854-8.

38. Young, C., Taylor, A. M., Owens, C. M. (2011). Paediatric cardiac computed tomography: A review of imaging techniques and radiation dose consideration. *European Radiology, 21(3),* 518–529. DOI 10.1007/s00330-010-2036-8.

39. Zheng, M., Zhao, H., Xu, J., Wu, Y., Li, J. (2013). Image quality of ultra-low-dose dual-source CT angiography using high-pitch spiral acquisition and iterative reconstruction in young children with congenital heart disease. *Journal of Cardiovascular Computed Tomography, 7(6),* 376–382. DOI 10.1016/j.jcct.2013.11.005.

40. Han, B. K., Lindberg, J., Overman, D., Schwartz, R. S., Grant, K. et al. (2012). Safety and accuracy of dual-source coronary computed tomography angiography in the pediatric population. *Journal of Cardiovascular Computed Tomography, 6(4),* 252–259. DOI 10.1016/j.jcct.2012.01.004.

41. Han, B. K., Lindberg, J., Grant, K., Schwartz, R. S., Lesser, J. R. (2011). Accuracy and safety of high pitch computed tomography imaging in young children with complex congenital heart disease. *American Journal of Cardiology, 107(10),* 1541–1546. DOI 10.1016/j.amjcard.2011.01.065.

42. Han, B. K., Grant, K. L., Garberich, R., Sedlmair, M., Lindberg, J. et al. (2012). Assessment of an iterative reconstruction algorithm (SAFIRE) on image quality in pediatric cardiac CT datasets. *Journal of Cardiovascular Computed Tomography, 6(3),* 200–204. DOI 10.1016/j.jcct.2012.04.008.

43. IAEA (2013). Scientific annex B: Effects of radiation exposure of children. Vol. 2, *Sources, effects and risks of ionizing radiation*. UNSCEAR 2013 Report. Ebook.

44. Guo, B. J., Yang, Z. L., Zhang, L. J. (2018). Gadolinium deposition in brain: Current scientific evidence and future perspectives. *Frontiers in Molecular Neuroscience, 11,* 1859. DOI 10.3389/fnmol.2018.00335.

45. Baumgartner, H., De Backer, J., Babu-Narayan, S. V., Budts, W., Chessa, M. et al. (2020). ESC Guidelines for the management of adult congenital heart disease. *European Heart Journal, 31,* 2915–2957, Advance online publication.

46. Di Salvo, G., Miller, O., Babu Narayan, S., Li, W., Budts, W. et al. (2018). Imaging the adult with congenital heart disease: A multimodality imaging approach-position paper from the EACVI. *European Heart Journal— Cardiovascular Imaging, 19(10),* 1077–1098. DOI 10.1093/ehjci/jey102.

47. Stout, K. K., Daniels, C. J., Aboulhosn, J. A., Bozkurt, B., Broberg, C. S. et al. (2019). AHA/ACC guideline for the management of adults with congenital heart disease: Executive summary: A report of the american college of cardiology/american heart association task force on clinical practice guidelines. *Circulation, 139(14),* e637–e697.